Latin American Journal of Solids and Structures
www.lajss.org

Analysis of Continuous and Discontinuous Cases of a Contact Problem Using Analytical Method and FEM

Abstract

In this paper, continuous and discontinuous cases of a contact problem for two elastic layers supported by a Winkler foundation are analyzed using both analytical method and finite element method. In the analyses, it is assumed that all surfaces are frictionless, and only compressive normal tractions can be transmitted through the contact areas. Moreover, body forces are taken into consideration only for layers. Firstly, the problem is solved analytically using theory of elasticity and integral transform techniques. Then, the finite element analysis of the problem is carried out using ANSYS software program. Initial separation distances between layers for continuous contact case and the size of the separation areas for discontinuous contact case are obtained for various dimensionless quantities using both solutions. In addition, the normalized contact pressure distributions are calculated for both cases. The analytical results are verified by comparison with finite element results. Finally, conclusions are presented.

Keywords

Continuous contact, discontinuous contact, finite element method, initial separation distance.

Ahmet Birinci [a]
Gökhan Adıyaman [b]
Murat Yaylacı [c]
Erdal Öner [d]

[a] Karadeniz Technical University, Department of Civil Engineering, e-mail: birinci@ktu.edu.tr
[b] Karadeniz Technical University, Department of Civil Engineering, e-mail: gadiyaman@hotmail.com
[c] Recep Tayyip Erdoğan University, Department of Civil Engineering, e-mail: murat.yaylaci@erdogan.edu.tr
[d] Bayburt University, Department of Civil Engineering, e-mail: eoner@bayburt.edu.tr

http://dx.doi.org/10.1590/1679-78251574

Received 10.09.2014
In Revised Form 16.01.2015
Accepted 16.02.2015
Available online 07.02.2015

1 INTRODUCTION

Since contact problems have different application areas in structural mechanics such as railways, foundation grillages, rolling mills, pavements of highway and airfield etc. (see, for example, Garrido and Lorenzana, 1998; Comez et al., 2004; Kahya et al. 2007), there has been an increasing attention on the contact problems. There is a large body of literature associated with contact problems both analytically (Keer et al., 1972; Weitsman, 1972; Ratwani and Erdogan, 1973; Gladwell, 1976;

Civelek et al., 1978; Geçit, 1986; Nowell and Hills, 1988; Porter and Hills, 2002) and numerically (Chan and Tuba, 1971; Francavilla and Zienkiewicz, 1975; Jing and Liao, 1990; Garrido et al., 1991).

Apart from these papers, Abdou and Salama (2004) studied the Fredholm integral equation of the second kind which obtained from the three-dimensional contact problem in the theory of elasticity with a generalized potential kernel. Haslingera and Vlachb (2006) analyzed discrete contact problems with Columb friction and found a solution dependent to coefficient of friction. El-Borgi et al. (2006) considered the plane problem of a receding contact between a functionally graded elastic layer and a homogeneous half-space when the two bodies were pressed together. A weighted residual relationship for the contact problem with Coulomb friction was carried out by Le van and Nguyen (2009).

Comez (2010) investigated frictional contact problem for a rigid cylindrical stamp and an elastic layer resting on a half plane. The axisymmetric problem of a frictionless double receding contact between a rigid stamp of axisymmetric profile, a functionally graded elastic layer and a homogeneous half space was studied by Rhimi et al. (2011). Zhang et al. (2012) reported a finite element model for 2D elastic-plastic contact analysis of multiple cosserat materials. Long and Wang (2013) investigated effects of surface tension on axisymmetric Hertzian contact problem. Yang (2013) studied solutions of dissimilar material contact problems. Chidlow and Teodorescu (2013) examined the frictionless two-dimensional contact problem of an inhomogeneously elastic material under a rigid punch. Zozulya (2013) presented comparative study of time and frequency domain BEM approaches in frictional contact problem for antiplane crack under harmonic loading. Öner and Birinci (2014) solved continuous contact problem for two elastic layers resting on an elastic half-infinite plane. A quadratic meshless boundary element formulation for isotropic damage analysis of contact problems with friction was examined by Gun (2014). An axisymmetric Hertzian contact problem of a rigid sphere pressing into an elastic half-space under cyclic loading was investigated by Kim and Jang (2014). A theoretical model of a frictional sliding contact problem for monoclinic piezoelectric materials under triangular and cylindrical punches was studied out by Zhou and Lee (2014).

When the literature is researched, it can be seen that there are not enough studies about contact problems with regard to existing body forces. Additionally, in the existing literature, although there are extensive studies on solution of contact problems both analytically and numerically, comparison of these methods in contact mechanics has not been explored completely. So, the aim of this paper is to present a comparative study of continuous and discontinuous cases of a contact problem using analytical method and FEM. In the following sections, firstly, the analytical solution of the problem is investigated. Secondly, the finite element analysis of the problem is examined. Then these two methods are compared to each other using various numerical problems. Finally conclusions are given.

2 ANALYTICAL SOLUTION OF THE PROBLEM

Consider the plane-strain contact problem (symmetric with respect to the y-axis) entailing two elastic layers supported by a Winkler foundation as shown in Figures (1a) and (1b). Layers are isotropic, homogeneous and linearly elastic. Symmetrical distributed load whose length 2a is subjected

to Layer 2. In the analyses, it is assumed that all surfaces are frictionless, and only normal tractions can be transmitted across the contact surfaces. Since every material has a weight in nature and including body forces approaches the solution to reality, body forces of the elastic layers are taken into account. Including body forces also converts the type of the problem from receding contact to continuous or discontinuous contact problem. Due to symmetry about y-axis, it is sufficient to consider only one-half of the problem geometry. Where applicable, the germane quantities are reckoned per unit length in the z- direction. Analytical solution of the problem is obtained using theory of elasticity and integral transform technique.

In the absence of body forces, the stress and the displacement components for Layer 1 and Layer 2 may be obtained as (Birinci and Erdol, 2003)

$$u_{ih}(x,y)=\frac{2}{\pi}\int_0^\infty\left\{\left[A_i+B_i y\right]e^{-\alpha y}+\left[C_i+D_i y\right]e^{\alpha y}\right\}\sin(\alpha x)\,d\alpha \tag{1}$$

$$v_{ih}(x,y)=\frac{2}{\pi}\int_0^\infty\left\{\left[A_i+B_i\left(\frac{\chi_i}{\alpha}+y\right)\right]e^{-\alpha y}+\left[-C_i+D_i\left(\frac{\chi_i}{\alpha}-y\right)\right]e^{\alpha y}\right\}\cos(\alpha x)\,d\alpha \tag{2}$$

$$\frac{1}{2\mu_i}\sigma_{ixh}(x,y)=\frac{2}{\pi}\int_0^\infty\left\{\left[\alpha\left(A_i+B_i y\right)-\left(\frac{3-\chi_i}{2}\right)B_i\right]e^{-\alpha y}+\left[\alpha\left(C_i+D_i y\right)+\left(\frac{3-\chi_i}{2}\right)D_i\right]e^{\alpha y}\right\}\cos(\alpha x)\,d\alpha \tag{3}$$

$$\frac{1}{2\mu_i}\sigma_{iyh}(x,y)=\frac{2}{\pi}\int_0^\infty\left\{-\left[\alpha\left(A_i+B_i y\right)+\left(\frac{1+\chi_i}{2}\right)B_i\right]e^{-\alpha y}+\left[-\alpha\left(C_i+D_i y\right)+\left(\frac{1+\chi_i}{2}\right)D_i\right]e^{\alpha y}\right\}\cos(\alpha x)\,d\alpha \tag{4}$$

$$\frac{1}{2\mu_i}\tau_{ixyh}(x,y)=\frac{2}{\pi}\int_0^\infty\left\{-\left[\alpha\left(A_i+B_i y\right)+\left(\frac{\chi_i-1}{2}\right)B_i\right]e^{-\alpha y}+\left[\alpha\left(C_i+D_i y\right)-\left(\frac{\chi_i-1}{2}\right)D_i\right]e^{\alpha y}\right\}\sin(\alpha x)\,d\alpha \tag{5}$$

where subscript h indicates the case without body forces. u=u(x,y) and v=v(x,y) are the x- and y-components of the displacement vector, respectively. $\sigma_x(x,y)$, $\sigma_y(x,y)$ and $\tau_{xy}(x,y)$ are the stress components of the layers. χ_i is an elastic constant and equals $\chi_i=(3-4\nu_i)$ for plane strain, μ_i is shear modulus, ν_i is Poisson's ratio (i=1,2). The subscripts 1 and 2 refer to the Layer 1 and Layer 2, respectively. A_i, B_i, C_i and D_i (i=1, 2) are unknown coefficients which will be determined from boundary conditions of the problem.

For the case in which body forces exist, the particular parts of σ_y stress components for Layer 1 and Layer 2 are obtained as (Birinci and Erdol, 2003)

$$\sigma_{1yp}(y)=-\rho_2 g h_2+\rho_1 g(y-h_1) \tag{6}$$

$$\sigma_{2yp}(y) = \rho_2 g(y - h) \tag{7}$$

where g, ρ_1 and ρ_2 are gravity acceleration, mass density of Layer 1 and mass density of Layer 2, respectively. Total field of displacements and stresses can be consequently written as

$$\sigma_{iy} = \sigma_{iyh} + \sigma_{iyp} \tag{8}$$

2.1 Continuous Contact Case

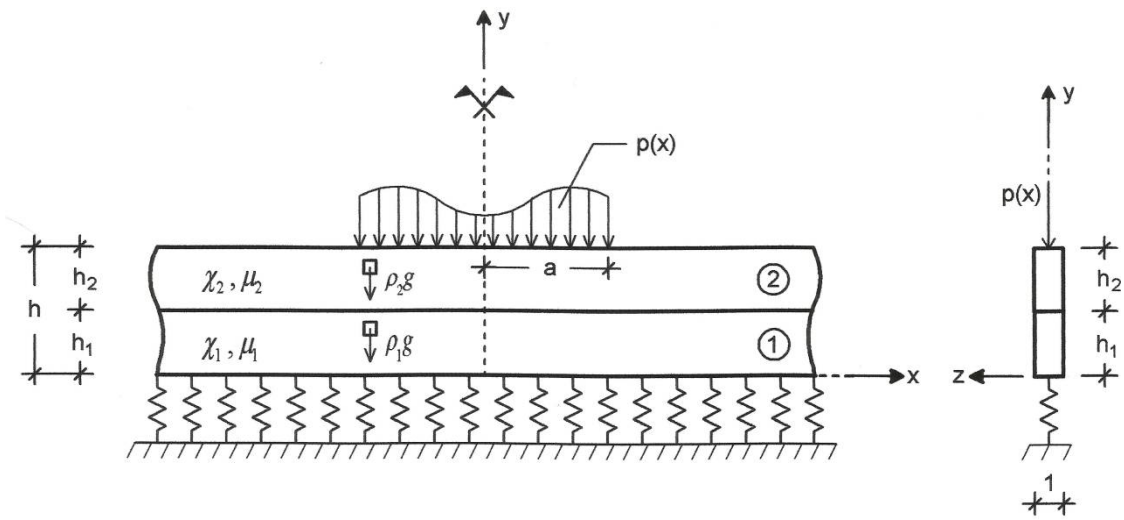

Figure 1a: Geometry of the problem related to continuous contact case.

If load factor defined as $\lambda = \dfrac{p(x)}{\rho_2 g h_2}$ is sufficiently small, then the contact between elastic layers, $y=h_1$, $0<x<\infty$, will be continuous, and A_i, B_i, C_i and D_i (i=1,2) must be determined from the following boundary conditions:

$$\tau_{2xy}(x,h) = 0 \qquad (0 \le x < \infty) \tag{9}$$

$$\tau_{2xy}(x,h_1) = 0 \qquad (0 \le x < \infty) \tag{10}$$

$$\tau_{1xy}(x,h_1) = 0 \qquad (0 \le x < \infty) \tag{11}$$

$$\tau_{1xy}(x,0) = 0 \qquad (0 \le x < \infty) \tag{12}$$

$$\sigma_{1y}\left(x,h_1\right)=\sigma_{2y}\left(x,h_1\right) \qquad \left(0\le x<\infty\right) \tag{13}$$

$$\sigma_{2y}\left(x,h\right)=\begin{Bmatrix}-p\left(x\right) & \left(0\le x<a\right)\\ 0 & \left(a\le x<\infty\right)\end{Bmatrix} \tag{14}$$

$$\sigma_{1y}(x,0)=k_0v_1(x,0) \qquad (0\le x<\infty) \tag{15}$$

$$\frac{\partial}{\partial x}\left[v_2\left(x,h_1\right)-v_1\left(x,h_1\right)\right]=0 \qquad \left(0\le x<\infty\right) \tag{16}$$

where k_0 is the stiffness of the Winkler foundation. By making use of boundary conditions (9-16), unknown A_i, B_i, C_i and D_i (i=1,2) constants can be determined. By substituting these constants into Eq. (8), after some simple manipulations, one may obtain the contact pressure along the interface $y=h_1$ as (Birinci and Erdol, 2003)

$$\begin{aligned}\sigma_y(x,h_1)=-\rho_2gh_2-\frac{4}{\pi}(1+\chi_2)\int_0^\infty\frac{P_j}{\Delta(\alpha)}e^{-\alpha h}e^{-\alpha h_1}Y1(\alpha)[4\alpha Y2(\alpha)\\ +k(1+\chi_1)Y3(\alpha)]\cos(\alpha x)d\alpha\end{aligned} \tag{17}$$

where

$$P_j=\int_0^\infty p(x)\cos(\alpha x)dx, \quad (j=1,2,3) \tag{18}$$

$$\begin{aligned}\Delta(\alpha)=Y4(\alpha)[-4\alpha(1+\chi_2)Y2(\alpha)-k(1+\chi_1+\chi_2+\chi_1\chi_2)Y3(\alpha)]\\ +\frac{\mu_2}{\mu_1}Y5(\alpha)[4\alpha(1+\chi_1)Y3(\alpha)+k(1+2\chi_1+{\chi_1}^2)Y6(\alpha)]\end{aligned} \tag{19}$$

$$Y1(\alpha)=e^{-2\alpha h_1}-e^{-2\alpha h}+(\alpha h-\alpha h_1)(e^{-2\alpha h_1}+e^{-2\alpha h}) \tag{20a}$$

$$Y2(\alpha)=1-e^{-2\alpha h_1}(2+4\alpha^2{h_1}^2-e^{-2\alpha h_1}) \tag{20b}$$

$$Y3(\alpha)=-1+e^{2\alpha h_1}(4\alpha h_1+e^{2\alpha h_1}) \tag{20c}$$

$$Y4(\alpha) = e^{-4\alpha h} - e^{-4\alpha h_1} - 2e^{-2\alpha h_1} e^{-2\alpha h}(2\alpha h - 2\alpha h_1) \tag{20d}$$

$$Y5(\alpha) = e^{-4\alpha h} - e^{-4\alpha h_1} - e^{-2\alpha h_1} e^{-2\alpha h}(2 + 4\alpha^2 h^2 + 4\alpha^2 h_1^{\,2} - 8\alpha^2 h h_1) \tag{20e}$$

$$Y6(\alpha) = 1 - e^{2\alpha h_1}(2 - e^{2\alpha h_1}) \tag{20f}$$

$$k = \frac{k_0}{\mu_1} \tag{21}$$

In this study, three different loading cases are considered. For each loading case, P_j (j=1,2,3) can be determined as

- Case 1: $p(x) = p_0 = \text{constant}$

$$P_1 = \frac{p_0}{\alpha}\sin(\alpha a) \tag{22}$$

- Case 2: $p(x) = p_0(1 - \frac{x^2}{a^2})$

$$P_2 = \frac{2p_0}{\alpha^3 a^2}\left[\sin(\alpha a) - \alpha a\cos(\alpha a)\right] \tag{23}$$

- Case 3: $p(x) = p_0(1 - \frac{x}{a})$

$$P_3 = \frac{p_0}{\alpha^2 a}\left[1 - \cos(\alpha a)\right] \tag{24}$$

Equating $\sigma_y(x, h_1)$ in Eq. (17) to zero after replacing $\omega = \alpha h$, $r = h_1 / h$, the expression in which x_{cr} (initial separation distance) will be obtained can be written as

$$\frac{1}{\lambda_{cr}} = -\frac{4}{\pi}(1 + \chi_2)\int_0^\infty \frac{f_j(\omega, a/h)}{\Delta(\omega, r)} e^{-\omega} e^{-\omega r} Y1(\omega, r)[4\frac{\omega}{h} Y2(\omega, r) + k(1 + \chi_1) Y3(\omega, r)]\cos(\omega \frac{x}{h}) d\omega \tag{25}$$

where f_j equals to corresponding loading P_j (j=1,2,3) given in Eqs. (22-24), λ_{cr} is critical load factor and it can be written as

$$\lambda_{cr} = \frac{p_{cr}}{\rho_2 g h_2} \tag{26}$$

After substituting $f_j(\omega, a/h)$ (j=1,2,3) values into Eq. (25) and solving the integral numerically, x_{cr} values, for which initial separation takes place may be obtained for various dimensionless quantities.

2.2 Discontinuous Contact Case

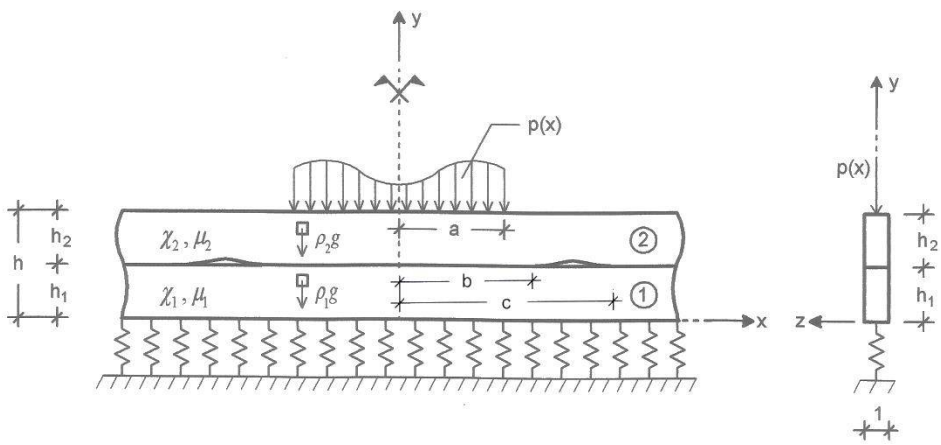

Figure 1b: Geometry of the problem related to discontinuous contact case.

Since the interface can't carry tensile tractions for $\lambda > \lambda_{cr}$, there will be a separation between the elastic layers in the neighborhood of $x = x_{cr}$ on the contact plane $y = h_1$. Assuming that the separation region is described by $b < x < c$ and $y = h_1$, boundary conditions for the discontinuous contact case are as follows

$$\tau_{2xy}(x,0) = 0 \qquad (0 \le x < \infty) \tag{27}$$

$$\tau_{2xy}(x,h_1) = 0 \qquad (0 \le x < \infty) \tag{28}$$

$$\tau_{1xy}(x,h_1) = 0 \qquad (0 \le x < \infty) \tag{29}$$

$$\tau_{1xy}(x,0) = 0 \qquad (0 \le x < \infty) \tag{30}$$

$$\sigma_{1y}\left(x,h_1\right)=\sigma_{2y}\left(x,h_1\right) \qquad \left(0\le x<\infty\right) \tag{31}$$

$$\sigma_{2y}\left(x,h\right)=\begin{Bmatrix}-p\left(x\right) & \left(0\le x<a\right)\\ 0 & \left(a\le x<\infty\right)\end{Bmatrix} \tag{32}$$

$$\sigma_{1y}(x,0)=k_0v_1(x,0) \qquad \left(0\le x<\infty\right) \tag{33}$$

$$\sigma_y\left(x,h_1\right)=0 \qquad \left(b<x<c\right) \tag{34}$$

$$\frac{\partial}{\partial x}\left[v_2\left(x,h_1\right)-v_1\left(x,h_1\right)\right]=\varphi(x) \qquad \left(b<x<c\right) \tag{35}$$

where **b** and **c** are unknowns, and functions of λ . Note that the unknown function $\varphi(x)$ in Eq. (35) may be replaced by

$$\varphi(x)=0, \qquad (0\le x<b, \quad c<x<\infty) \tag{36}$$

and

$$\int_b^c\varphi(x)dx=0 \tag{37}$$

Utilizing the boundary conditions (27-33) and (35), the new constants A_i, B_i, C_i and D_i (i=1,2) which appear in Eqs. (1-5) may be obtained in terms of the unknown function $\varphi(x)$. Then, Eq. (34) gives the following singular integral equation which $\varphi(x)$ is the unknown function:

$$\frac{4\mu_1}{(1+\chi_1)\rho_2gh_2}\frac{1}{(1+m)}\frac{1}{\pi}\int_b^c\left[\frac{1}{t+x}+\frac{1}{t-x}+k_1(x,t)\right]\varphi(t)dt-\frac{4}{\pi}\lambda k_2(x)=1 \tag{38}$$

where

$$\begin{aligned}k_1(x,t)=\int_0^\infty\Bigg\{&\frac{1}{\Delta(\alpha)}\left(1+\frac{1}{m}\right)(1+\chi_2)\left[4\alpha Y2(\alpha)+k(1+\chi_1)Y3(\alpha)\right]Y5(\alpha)-1\Bigg\}\\ &*\left\{\sin\left[\alpha(t+x)\right]+\sin\left[\alpha(t-x)\right]\right\}d\alpha\end{aligned} \tag{39}$$

$$k_2(x)=\int_0^\infty\left\{\frac{P_i}{\Delta(\alpha)}e^{-\alpha h}e^{-\alpha h_1}(1+\chi_2)Y1(\alpha)\left[4\alpha Y2(\alpha)+k(1+\chi_1)Y3(\alpha)\right]\right\}\cos(\alpha x)d\alpha \tag{40}$$

$$m = \frac{\mu_1}{\mu_2}\frac{1+\chi_2}{1+\chi_1} \tag{41}$$

One may notice that because of the smooth contact at the end points **b** and **c**, the function $\varphi(x)$ equals zero at the ends and the index of the integral Eq. (38) is equal to -1 (Erdogan and Gupta, 1972). The consistency condition of the integral Eq. (38) defined as

$$\int_b^c \left\{ \begin{array}{l} \dfrac{4\mu_1}{(1+\chi_1)\rho_2 g h_2}\dfrac{1}{(1+m)}\dfrac{1}{\pi}\displaystyle\int_b^c \left[\frac{1}{t+x}+\frac{1}{t-x}+k_1(x,t)\right]\varphi(t)dt \\ -1-\dfrac{4}{\pi}\lambda k_2(x) \end{array} \right\} \frac{dx}{\left[(x-b)(c-x)\right]^{1/2}} = 0 \tag{42}$$

Defining the following dimensionless quantities,

$$\eta = \frac{2t}{c-b} - \frac{c+b}{c-b} \tag{43}$$

$$\xi = \frac{2x}{c-b} - \frac{c+b}{c-b} \tag{44}$$

$$g(\eta) = \varphi(t)\frac{4\mu_1}{(1+\chi_1)\rho_2 g h_2} \tag{45}$$

and substituting Eqs. (43-45) into the integral Eq. (38), the single-value condition (37), and the consistency condition (42), the following equations are obtained:

$$\frac{1}{1+m}\frac{1}{\pi}\int_{-1}^{1}\left[\frac{1}{\eta-\xi}+\frac{1}{\eta+\xi+2\dfrac{c+b}{c-b}}+\frac{c-b}{2h}k_1^{*}(\xi,\eta)\right]g(\eta)d\eta = \frac{4}{\pi}\lambda k_2^{*}(\xi)+1 \tag{46}$$

$$\int_{-1}^{1} g(\eta)d\eta = 0 \tag{47}$$

$$\int_{-1}^{1}\frac{d\xi}{(1-\xi^2)^{1/2}}\left\{1+\frac{4}{\pi}\lambda k_2^{*}(\xi)-\frac{1}{1+m}\frac{1}{\pi}\int_{-1}^{1}\left[\frac{1}{\eta+\xi+2\dfrac{c+b}{c-b}}+\frac{c-b}{2h}k_1^{*}(\xi,\eta)\right]g(\eta)d\eta\right\} = 0 \tag{48}$$

where

$$k_1^*(\xi,\eta) = k_1^*(x,t) \text{ and } k_2^*(\xi) = k_2^*(x) \tag{49a-49b}$$

and in which

$$\begin{aligned} k_1^*(x,t) = \int_0^\infty & \left\{ \frac{1}{\Delta(\omega,r)} \left(1+\frac{1}{m}\right)(1+\chi_2)\left[4\frac{\omega}{h} Y2(\omega,r) + k(1+\chi_1)Y3(\omega,r)\right] Y5(\omega,r) - 1 \right\} \\ & * \left\{ \sin\left[\frac{\omega}{h}(t+x)\right] + \sin\left[\frac{\omega}{h}(t-x)\right] \right\} d\omega \end{aligned} \tag{50}$$

$$k_2^*(x) = \int_0^\infty \left\{ \begin{aligned} & \frac{f_i(\omega, a/h)}{\Delta(\omega,r)} e^{-\omega} e^{-\omega,r} (1+\chi_2) Y1(\omega,r) \\ & * \left[4\frac{\omega}{h} Y2(\omega,r) + k(1+\chi_1) Y3(\omega,r) \right] \end{aligned} \right\} \cos(\omega \frac{x}{h}) d\omega \tag{51}$$

To insure smooth contact at the end points of the separation area, let

$$g(\eta) = G(\eta)(1-\eta^2)^{1/2}, \qquad (-1 < \eta < 1) \tag{52}$$

Using the appropriate Gauss-Chebyshev integration formula (Erdogan and Gupta), Eqs. (46) and (47) become

$$\sum_{k=1}^{n} \frac{1-\eta_k^2}{n+1} \left\{ \frac{1}{1+m} \left[\begin{aligned} & \frac{1}{\eta_k - \xi_j} + \frac{1}{\eta_k + \xi_j + 2\dfrac{c+b}{c-b}} \\ & + \frac{c-b}{2h} k_1^*(\xi_j, \eta_k) \end{aligned} \right] G(\eta_k) \right\} = \frac{4}{\pi} \lambda k_2^*(\xi_j) + 1 \qquad (j = 1,\ldots,n+1) \tag{53}$$

$$\sum_{k=1}^{n} \frac{1-\eta_k^2}{n+1} G(\eta_k) = 0 \tag{54}$$

where

$$\eta_k = \cos\left(\frac{k\pi}{n+1}\right) \qquad (k = 1,\ldots,n) \tag{55}$$

$$\xi_j = \cos\left(\frac{\pi}{2}\frac{2j-1}{n+1}\right) \qquad (j = 1,\ldots,n+1) \tag{56}$$

Eqs. (53) and (54) give (n+2) equations in order to determine (n+2) unknowns namely $G(\eta_k)$, $(k = 1,\ldots,n)$, b and c. However, since the equations are nonlinear in b and c, an iterative scheme has

to be used in order to obtain these unknowns. In this iterative procedure, firstly (n) equations [j=1,...,(n/2),(n/2+2),...,(n+1)] are chosen from Eq. (53) and the remaining one [j=n/2+1] is kept as the stopping criteria along with single-value condition (54).

After predicting values for **b** and **c**, $G(\eta_k)$ are calculated using previously determined (n) equations. If the chosen **b** and **c** and obtained $G(\eta_k)$ values ensure the stopping criteria equations, the solution would have been found. Otherwise, $G(\eta_k)$ values are recalculated after predicting new **b** and **c** values.

Note that the consistency condition of the integral equation such as (48) is automatically satisfied. Also, Eq. (38) gives the stress $\sigma_y(x,h_1)$ outside as well as inside the separation region (b,c). Thus, once the unknowns $G(\eta_k)$, **b** and **c** are determined, the contact pressure may be easily evaluated for the discontinuous contact case.

3 FINITE ELEMENT ANALYSIS OF THE PROBLEM

In this section, the problem has been studied by the finite element method (FEM) using a commercial package program ANSYS. ANSYS Multiphysics is a powerful interactive environment for modeling and solving all kinds of scientific and engineering problems based on partial differential equations (PDEs). To solve the PDEs, ANSYS Multiphysics uses the proven finite element method (FEM). The software runs the finite element analysis together with adaptive meshing and error control using a variety of numerical solvers (Biswas and Banerjee, 2013).

The problem is considered as a two-dimensional contact problem and the material of the layers are assumed elastic and isotropic. The physical system under consideration exhibits symmetry in geometry, material properties and loading. Due to the symmetry of the problem, only one half of the geometry of the problem is to be modeled. The geometry and the applied load are shown schematically in Fig. 2 and Finite Element model of the problem before analysis is shown in Fig. 3. In the study, two dimensional solid elements (PLANE 183) are used to model the layers. The PLANE 183 element is defined by six nodes having two degrees of freedom at each node: translations in the nodal x and y directions. The element may be used as a plane element (plane stress, plane strain and generalized plane strain). Winkler foundation is modelled by linear spring element (COMBIN 14). The COMBIN14 element or the longitudinal element spring-damper option is a uniaxial tension-compression element with up to two degrees of freedom at each node: translations in the nodal x and y directions. No bending or torsion is considered. If damping is neglected, the spring element will simply represent the linear Winkler model of one parameter which is the simple model to represent soil (Al- Azzawi et al., 2010).

The contact region is meshed by Surface-to-Surface CONTA172 and TARGE169 contact elements. CONTA172 is used to represent that of the mechanical contact analysis. The target surface, defined by TARGE169, was therefore used to represent 2-D "target" surfaces for the associated contact elements CONTA172. Plane strain finite elements are used for the meshing of the entire geometry. Frictionless surface-to-surface contact elements are used to model the interaction between the contact surfaces and Augmented Lagrangian method is used as the contact algorithm.

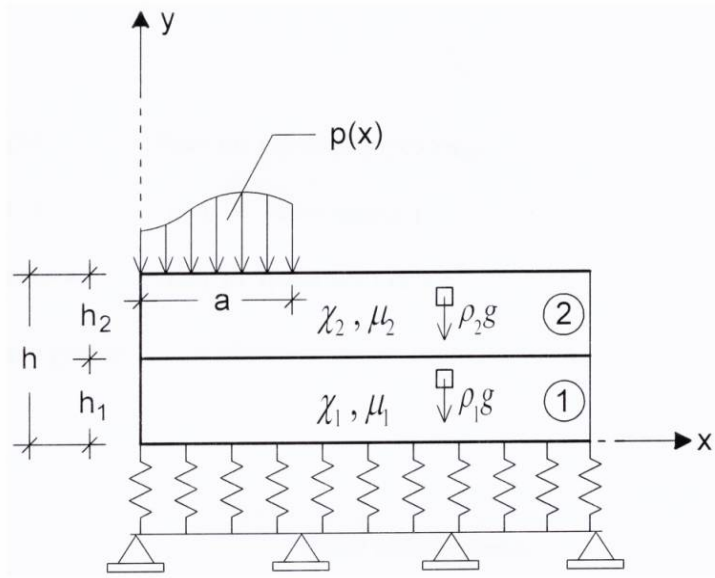

Figure 2: The geometry of the problem for finite element analysis.

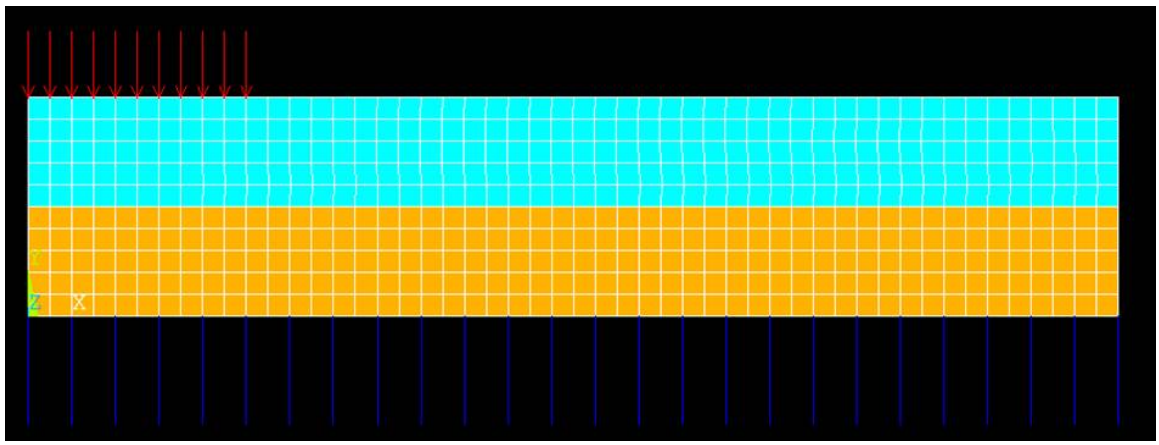

Figure 3: Finite element model of the problem before analysis.

4 COMPARISON AND VERIFICATION OF ANALYTICAL AND FINITE ELEMENT APPROACHES

In this section, by using the described methods in the previous sections, initial separation distances between layers for continuous contact case, the size of the separation areas for discontinuous contact case, and the normalized contact pressure distributions for both contact cases are given for various dimensionless quantities such as $k = k_0 / \mu_1$, μ_2 / μ_1 , h_1 / h and λ . Additionally, the results obtained using FEM have been compared and verified with analytical results.

The effects of μ_2/μ_1 and $k = k_0/\mu_1$ on the initial separation distance for continuous contact case are presented in Table 1. It demonstrates that the initial separation distance increases with increasing of μ_2/μ_1. This means that as Layer 2 becomes more rigid compared to Layer 1, the initial separation occurs at a more distant point from the axis of symmetry. Moreover, increasing stiffness of the Winkler foundation ($k = k_0/\mu_1$) reduces the value of initial separation distance x_{cr} and the initial separation occurs at a point closer to the axis of symmetry. As $k = k_0/\mu_1$ increases, the change of initial separation distance x_{cr} dwindles away and x_{cr} approaches to a constant value.

	$\mu_2/\mu_1 = 0.575$			$\mu_2/\mu_1 = 1$			$\mu_2/\mu_1 = 1.74$		
k $\downarrow$	x_{cr}/h			x_{cr}/h			x_{cr}/h		
	Analytical	FEM	Error (%)	Analytical	FEM	Error (%)	Analytical	FEM	Error (%)
0.01	6.7840	6.750	0.50	7.1842	7.125	0.82	7.7506	7.750	0.01
0.05	4.6646	4.700	0.76	4.9258	4.875	1.03	5.2968	5.300	0.06
0.1	4.0054	4.000	0.14	4.2210	4.250	0.69	4.5282	4.500	0.62
0.5	2.9086	2.900	0.30	3.0530	3.050	0.10	3.2510	3.250	0.03
1	2.5474	2.550	0.10	2.7010	2.700	0.04	2.8770	2.875	0.07
2	2.2408	2.250	0.41	2.4182	2.400	0.75	2.5872	2.575	0.47
5	2.0174	2.000	0.86	2.1700	2.150	0.92	2.3254	2.300	1.09
10	1.9418	1.950	0.42	2.0684	2.050	0.89	2.2088	2.200	0.40
50	1.8770	1.875	0.11	1.977	2.000	1.16	2.0972	2.100	0.13
100	1.8682	1.865	0.17	1.9646	1.975	0.53	2.0818	2.075	0.33
$\rightarrow\infty$	1.8594	1.850	0.51	1.9520	1.950	0.10	2.0658	2.050	0.76

Table 1: Variation of the initial separation distance x_{cr} with μ_2/μ_1 for various values of $k = k_0/\mu_1$ ($a/h = 1$, $h_1/h = 0.5$, $p(x) = p_0$).

Figure 4 illustrates that the effect of stiffness of the Winkler foundation on the normalized contact pressure between layers for continuous contact case. The results of this figure reveal that maximum normalized contact pressure occurs at the axis of symmetry and maximum normalized contact pressure and initial separation distance decrease with increasing of $k = k_0/\mu_1$. Table 2 depicts that the effect of different loading cases on the initial separation distance x_{cr}. Examination of Table 2 indicates that maximum initial separation distance is obtained from loading case 1 [$p(x) = p_0$ =constant].

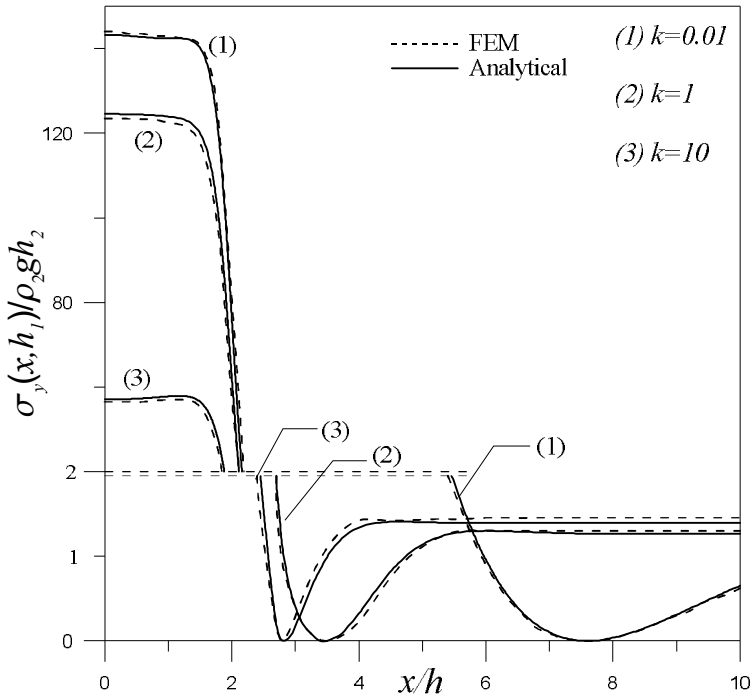

Figure 4: Effect of stiffness of the Winkler foundation on the normalized contact pressure between layers for continuous contact case ($a/h = 2,\ \mu_2/\mu_1 = 0.75,\ h_1/h = 0.6,\ \ p(x) = p_0$).

p(x) ↓	x_{cr}/h		
	Analytical	FEM	Error (%)
p_0	3.34	3.35	0.30
$p_0(1-x^2/a^2)$	2.86	2.85	0.35
$p_0(1-x/a)$	2.76	2.75	0.36

Table 2: Effect of different loading cases on the initial separation distance x_{cr} ($a/h = 2,\ \mu_2/\mu_1 = 0.75,\ \ h_1/h = 0.6$) .

Fig. 5 presents the effect of different loading cases on the normalized contact pressure between layers for continuous contact case. As seen in Fig. 6, Maximum normalized contact pressure between layers is obtained from loading case 3 $[p(x) = p_0(1 - \frac{x}{a})]$.

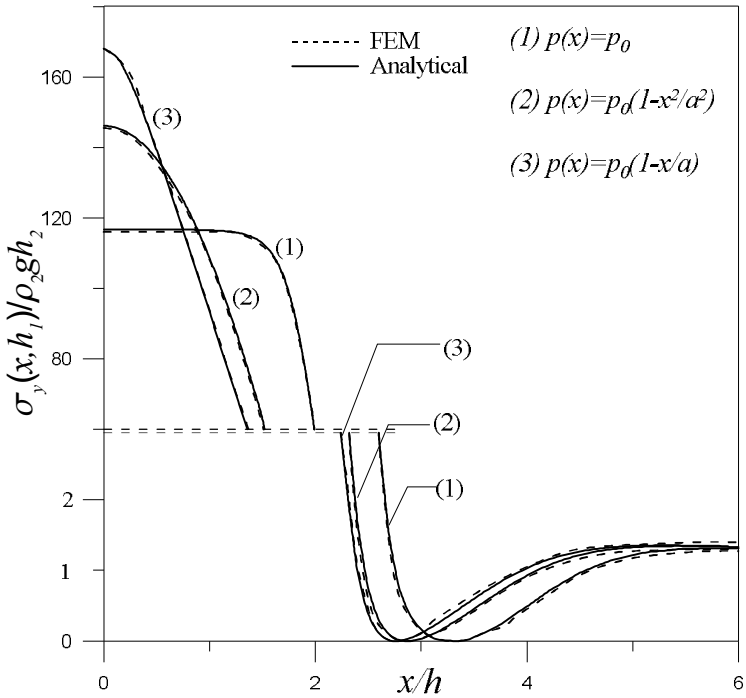

Figure 5: Effect of different loading cases on the normalized contact pressure between layers for continuous contact case ($a/h = 2,\ \mu_2/\mu_1 = 0.75,\ h_1/h = 0.6$).

Tables 3 and 4 show the influence of h_1/h on separation distances (b and c) for different loading cases in the case of discontinuous contact. It can be concluded from Tables 3 and 4 that increasing the value of h_1/h results in a decrease of separation distances (b and c) between the layers for both loading cases $[p(x) = p_0[1-(x/a)]$ and $p(x) = p_0]$.

h_1/h ↓	b/h			c/h			(c−b)/h		
	Analytical	FEM	Error (%)	Analytical	FEM	Error (%)	Analytical	FEM	Error (%)
0.30	1.5525	1.56	0.48	2.6712	2.68	0.33	1.1187	1.12	0.12
0.40	1.4919	1.48	0.80	2.4794	2.48	0.02	0.9875	1	1.26
0.50	1.4366	1.43	0.46	2.2312	2.23	0.05	0.7946	0.8	0.68
0.60	1.3985	1.40	0.11	1.8460	1.85	0.22	0.4475	0.45	0.56

Table 3 : The effect of h_1/h on separation distances (b and c) for loading case 3 in the case of discontinuous contact ($a/h = 1,\ p(x) = p_0[1-(x/a)],\ \mu_2/\mu_1 = 0.575,\ k = 5,\ \lambda = 150$).

h_1/h ↓	b/h			c/h			$(c-b)/h$		
	Analytical	FEM	Error (%)	Analytical	FEM	Error (%)	Analytical	FEM	Error (%)
0.30	1.6330	1.63	0.18	4.1600	4.14	0.48	2.5270	2.51	0.67
0.40	1.5698	1.58	0.65	3.8006	3.80	0.02	2.2308	2.22	0.48
0.50	1.5084	1.50	0.56	3.3790	3.35	0.86	1.8706	1.85	1.10
0.60	1.4412	1.44	0.08	2.8335	2.82	0.48	1.3923	1.38	0.88

Table 4: The effect of h_1 / h on separation distances (b and c) for loading case 1 in the case of discontinuous contact ($a / h = 1$, $p(x) = p_0$, $\mu_2 / \mu_1 = 0.575$, $k = 5$, $\lambda = 150$).

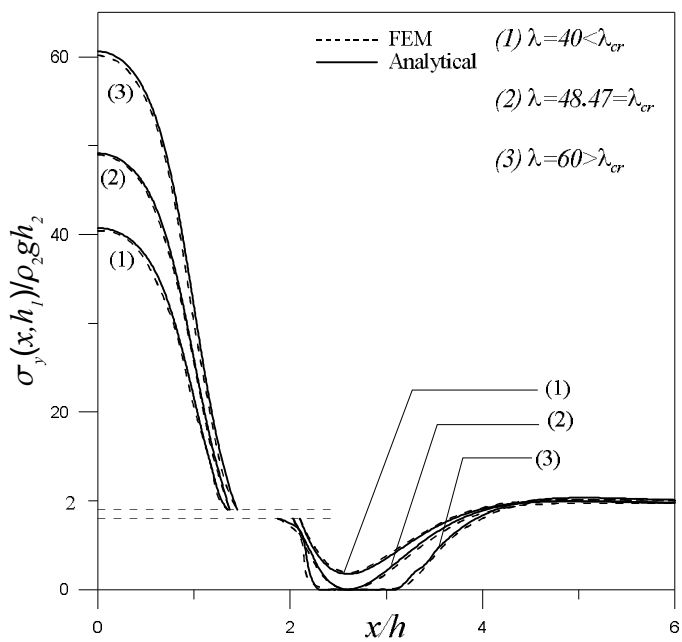

Figure 6: Normalized contact pressure distributions for continuous contact case ($\lambda \le \lambda_{cr}$) and discontinuous ($\lambda > \lambda_{cr}$) contact case ($a / h = 1$, $\mu_2 / \mu_1 = 0.575$, $h_1 / h = 0.4$, $k = 1$, $p(x) = p_0$).

The normalized contact pressure distributions for continuous contact case ($\lambda \le \lambda_{cr}$) and discontinuous ($\lambda > \lambda_{cr}$) contact case are depicted in Fig. 6. As seen in Fig. 6, there are three regions in the case of discontinuous contact. These are continuous contact region, separation zone and also continuous contact region where the effect of the external load decreases and disappears infinitely. Deformation shapes after finite element analysis related to Fig. 6 for continuous and discontinuous cases are shown in Fig. 7. Finally, the examination of all tables and figures shows that finite element solution indicates a good agreement with analytical solution.

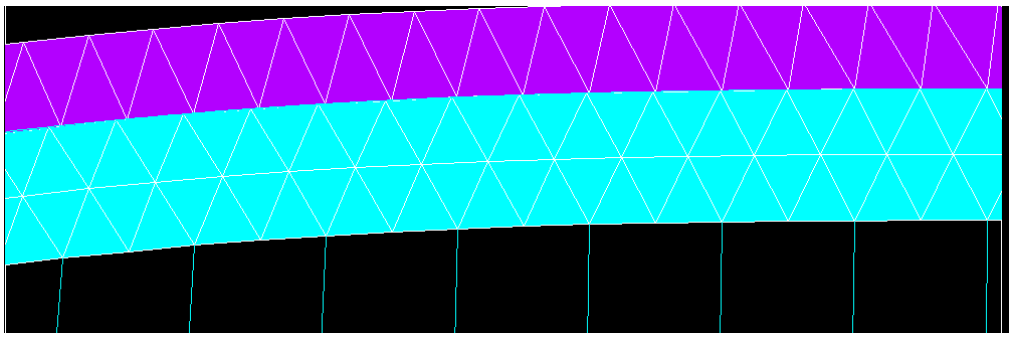

(a) Continuous contact case

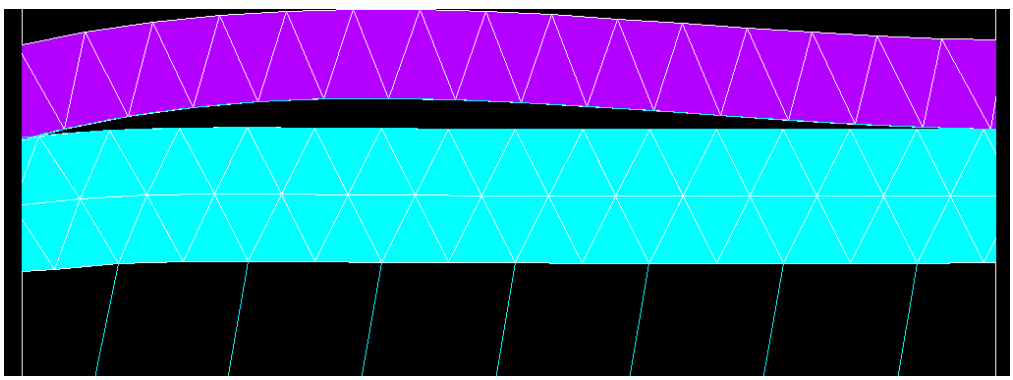

(b) Discontinuous contact case

Figure 7: Deformation shapes after finite element analysis for continuous contact case (a) and discontinuous contact case (b) related to Fig. 6.

5 CONCLUSIONS

The main purpose of this paper is to compare and verify results obtained using analytical method and FEM for a contact problem in the continuous and discontinuous contact cases. So, the problem is solved analytically using linear elasticity theory and integral transform technique. Then, initial finite element model of the problem is created by ANSYS software and finite element analysis is performed. According to this study, the followings can be deducted:

- Initial separation distance increases as $(k = k_0 / \mu_1)$ decreases.
- Increasing stiffness of the Winkler foundation $(k = k_0 / \mu_1)$ reduces the value of initial separation distance and the initial separation occurs at a point more close to the axis of symmetry.
- As $k = k_0 / \mu_1$ increases, the change of initial separation distance x_{cr} dwindles away and x_{cr} approaches to a constant value

- Initial separation distance increases with increasing of μ_2 / μ_1. This means that as Layer 2 becomes more rigid as against Layer 1, the initial separation occurs at more distant point from the axis of symmetry.
- Maximum normalized contact pressure occurs at the axis of symmetry and maximum normalized contact pressure and initial separation distance decrease with increasing of $k = k_0 / \mu_1$.
- Maximum initial separation distance is obtained from loading case 1 $[p(x) = p_0]$.
- Maximum normalized contact pressure between layers is obtained from loading case 3 $[p(x) = p_0(1 - \frac{x}{a})]$.
- Increasing the value of h_1 / h results in an decrease of separation distances (b and c) between the layers for both loading cases
- There are three regions in the case of discontinuous contact. These are continuous contact region, separation zone and also continuous contact region where the effect of the external load decreases and disappears infinitely
- It is observed that the results obtained using FEM is in a good agreement with the analytical results.

References

Abdou, M.A., Salama, F.A. (2004). Integral equation and contact problem, Applied Mathematics and Computation 149: 735–746.

Al- Azzawi, A.A., Mahdy, A.H., Farhan, O.S. (2010). Finite element analysis of deep beams on nonlinear elastic foundations, Journal of the Serbian Society for Computational Mechanics 4(2): 13-42.

ANSYS, (2007). Swanson Analysis Systems Inc., Houston PA, USA.

Birinci, A., Erdol, R. (2003). A frictionless contact problem for two elastic layers supported by a Winkler foundation, Structural Engineering and Mechanics 15(3): 331-344.

Biswas, P.K., Banerjee, S. (2013). ANSYS based fem analysis for three and four coil active magnetic bearing-a comparative study, International Journal of Applied Science and Engineering 11(3): 277-292.

Chan, S.K., Tuba, I.S. (1971). A finite element method for contact problems of solid bodies-1: Theory and validation, International Journal of Mechanical Sciences 13: 615–625.

Chidlow, S.J., Teodorescu, M. (2013). Two-dimensional contact mechanics problems involving inhomogeneously elastic solids split into three distinct layers, International Journal of Engineering Science 70: 102–123.

Civelek, M.B., Erdogan, F., Cakiroglu., A.O. (1978). Interface separation for an elastic layer loaded by a rigid stamp, International Journal of Engineering Science 16(9): 669–679.

Comez, I., Birinci, A., Erdol, R. (2004). Double receding contact problem for a rigid stamp and two layers, European Journal of Mechanics A/Solids 23: 301–309.

Comez, I. (2010). Frictional contact problem for a rigid cylindrical stamp and an elastic layer resting on a half plane, International Journal of Solids and Structures 47: 1090–1097.

El-Borgi, S., Abdelmoula, R., Keer, L. (2006). A receding contact plane problem between a functionally graded layer and a homogeneous substrate, International Journal of Solids and Structures 43: 658–674.

Erdogan, F., Gupta, G. (1972). On the numerical solutions of singular integral equations, Quarterly of Applied mathematics 29: 525-534.

Francavilla, A., Zienkiewicz, O.C. (1975). A note on numerical computation of elastic contact problems, International Journal for Numerical Methods in Engineering 9(4): 913–924.

Garrido, J.A., Foces, A., Paris, F. (1991). BEM applied to receding contact problems with friction, Mathematical and Computer Modelling 15: 143–154.

Garrido, J.A., Lorenzana, A. (1998). Receding contact problem involving large displacements using the BEM, Engineering Analysis with Boundary Elements 21: 295–303.

Geçit, M.R. (1986). Axisymmetric contact problem for a semi-infinite cylinder and a half space, International Journal of Engineering Science 24(8): 1245-1256.

Gladwell, G.M.L. (1976). On some unbonded contact problems in plane elasticity theory, Journal of Applied Mechanics 43(2): 263-267.

Gun, H. (2014). Isotropic damage analysis of frictional contact problems using quadratic meshless boundary element method, International Journal of Mechanical Sciences 80: 102–108.

Haslingera, J., Vlachb, O. (2006). Approximation and numerical realization of 2D contact problems with Coulomb friction and a solution-dependent coefficient of friction, Journal of Computational and Applied Mathematics 197: 421 – 436.

Jing, H.S., Liao, M.L. (1990). An improved finite element scheme for elastic contact problems with friction, Computers & Structures 35(5): 571–578.

Kahya, V., Ozsahin, T.S., Birinci, A., Erdol, R. (2007). A receding contact problem for an anisotropic elastic medium consisting of a layer and a half plane, International Journal of Solids and Structures 44: 5695– 5710.

Keer, L.M., Dundurs, J., Tsai, K.C. (1972). Problems involving of a receding contact between a layer and a half space, Journal of Applied Mechanics -T ASME 39: 1115-1120.

Kim, J.H., Jang, Y.H. (2014). Frictional Hertzian contact problems under cyclic loading using static reduction, International Journal of Solids and Structures 51: 252–258.

Le van, A., Nguyen, T.T.H. (2009). A weighted residual relationship for the contact problem with Coulomb friction, Computers & Structures 87: 1580–1601.

Long, J.M., Wang, G.F. (2013). Effects of surface tension on axisymmetric Hertzian contact problem, Mechanics of Materials 56: 65–70.

Nowell, D., Hills, D.A. (1988). Contact problems incorporating elastic layers, International Journal of Solids and Structures 24(1): 105-111.

Öner, E., Birinci, A. (2014). Continuous contact problem for two elastic layers resting on an elastic half-infinite plane, Journal of Mechanics of Materials and Structures 9(1): 105–119.

Porter, M.I., Hills, D.A. (2002). Note on the complete contact between a flat rigid punch and an elastic layer attached to a dissimilar substrate, International Journal of Mechanical Sciences 44: 509–520.

Ratwani, M., Erdogan, F. (1973). On the plane contact problem for a frictionless elastic layer, International Journal of Solids and Structures 9: 921-936.

Rhimi, M., El-Borgi, S., Lajnef, N. (2011). A double receding contact axisymmetric problem between a functionally graded layer and a homogeneous substrate, Mechanics of Materials 43: 787-798.

Weitsman, Y. (1972). A tensionless contact between a beam and an elastic half space, International Journal of Engineering Science 10: 73-81.

Yang, Y.Y. (2013). Solutions of dissimilar material contact problems, Engineering Fracture Mechanics 100: 92–107.

Zhang, H.W., Xie, Z.Q., Chen, B.S., Xing, H.L. (2012). A finite element model for 2D elastic-plastic contact analysis of multiple cosserat materials, European Journal of Mechanics A/Solids 31: 139-151.

Zhou, Y.T., Lee, K.Y. (2014). Investigation of frictional sliding contact problems of triangular and cylindrical punches on monoclinic piezoelectric materials, Mechanics of Materials 69: 237–250.

Zozulya, V. (2013). Comparative study of time and frequency domain BEM approaches in frictional contact problem for antiplane crack under harmonic loading, Engineering Analysis with Boundary Elements 37: 1499–1513.